Heliyon 10 (2024) e37004

Contents lists available at ScienceDirect

Heliyon

journal homepage: www.cell.com/heliyon

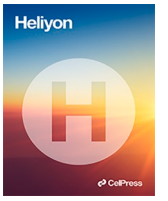

Research article

Temporal characteristics of turbulent flow and moth orientation behaviour patterns with fluent simulation and moth-based moving model simulation

Yanting Liu, Ryohei Kanzaki *

The University of Tokyo Research Center for Advanced Science and Technology, Komaba 4-6-1, Meguro-ku, 153-8904, Japan

ARTICLE INFO

Keywords:
Insect
Odour orientation
Model
Simulation
Turbulent flow
Reaction time

ABSTRACT

Objective: Previous research has explored the pheromone release patterns of female moths, revealing species-specific release frequencies and the transmission of temporal information through odourant plumes in turbulent flows. Varying the release frequency during the orientation process results in distinct orientation behaviours. Studies on moth movement patterns have determined that encounters and deviations from odour plumes elicit distinct reactions; the time interval between each movement pattern is measured as the "reaction time," and the interval between each detection and loss of odourant plume is measured as the "gap length."
Methods: We simulated turbulent flow at various release frequencies. Our efforts focused on establishing a model that could simulate the joint orientation movement under turbulent flow and intermittent plumes. We built an agent moving mechanism, including wind velocity information, with particular reference to the temporal parameter and orientation success efficiency.
Results: We calculated the time threshold of each burst in different simulations under different wind velocities and release frequencies. The time structure characteristics of the plume along the turbulent flow vary depending on the distance from the source. We simulated walking agents in a turbulent environment and recorded their behaviour processes. The reaction time, release interval, and time threshold were related to the orientation results.
Conclusion: On the basis of previous experimental results and our simulations, we conclude that the designated interval time likely enhances search efficiency. The complex and dynamic natural environment presents various opportunities for using this unique odour-source searching capability in different scenarios, potentially improving the control systems of odour-searching robots.

1. Introduction

The primary behaviours of insects involve searching for and locating odour sources. The orientation of insects is particularly notable because of their high sensitivity to both chemical and mechanical signals, as is evident from their navigational abilities [1]. Many insects navigate towards resources by following a windborne odour plume that is associated with the resource and then use specialized movement strategies to efficiently reach their destination. These search strategies are of significant interest to researchers studying effective navigation algorithms [2].

* Corresponding author.
E-mail address: kanzaki@rcast.u-tokyo.ac.jp (R. Kanzaki).

https://doi.org/10.1016/j.heliyon.2024.e37004
Received 7 December 2023; Received in revised form 22 August 2024; Accepted 26 August 2024
Available online 28 August 2024

Female moths release pheromones and interact with male moths for mating. The release strategies can be influenced by different conditions [3,4]. Previous studies have revealed that female moths emit sex pheromones in discrete pulses rather than in a continuous stream [5]. The emission rate of these pheromone pulses is approximately 1.5 pulses/s [6]. The release of pheromones by female silk moths occurs at a frequency of approximately 0.8 Hz [7]. When pheromones are released downwind, their concentration and components can change, resulting in the formation of spatial patterns along the length of the plume. Studies have shown that in natural environments, such as open fields and forests, the pheromone plume exhibits a temporal structure that extends beyond its source [8]. The proposed hypothesis suggests that this temporal patterned trail provides sequential orientation cues for approaching mates. In addition, the antennae of male moths may have enhanced functionality when exposed to pulsed plumes with chemical pulsation.

Previous studies have conducted experiments using two distinct pulsing tempos: 0.5 p/s and 1 p/s [9]. Male moths exhibited a higher flight response to point-source plumes and pulsed pheromone clouds than to continuous presentation or clean air conditions.

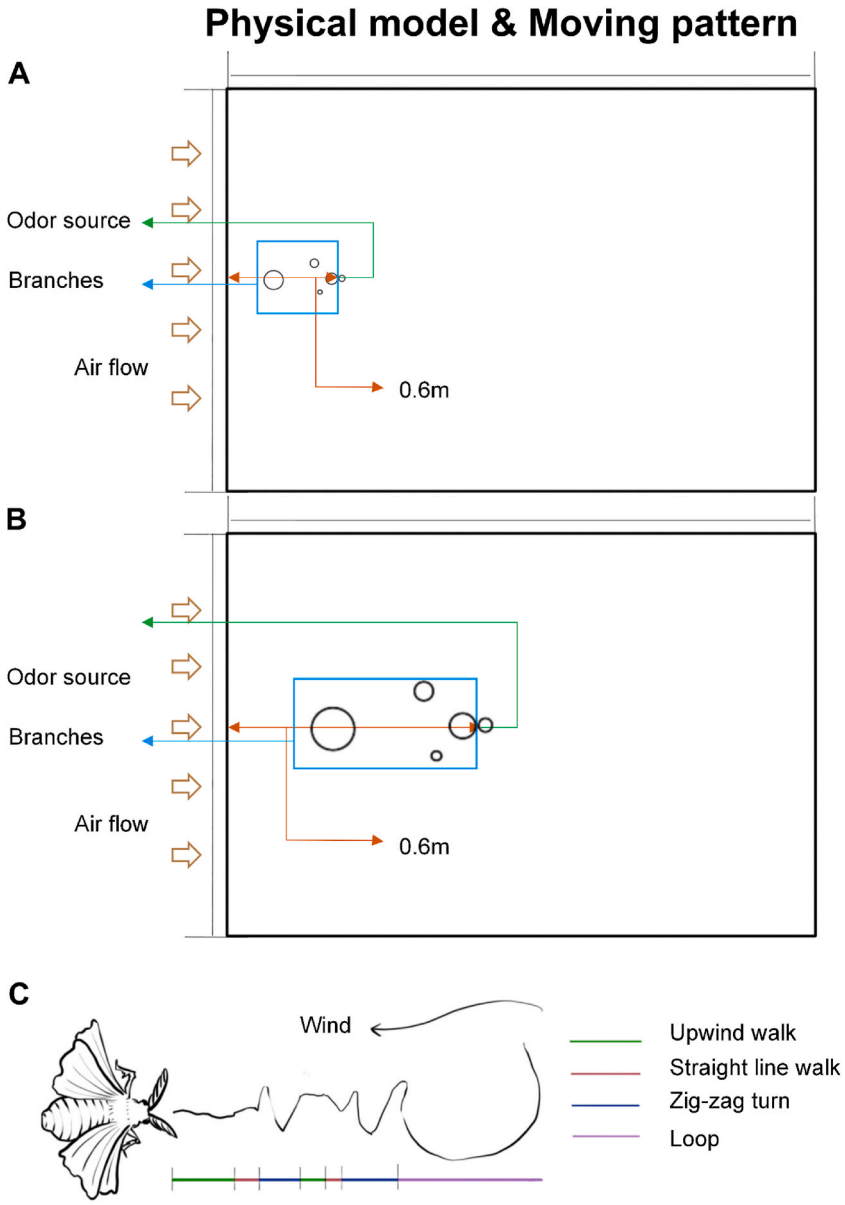

Fig. 1. Physical construction of the turbulent simulation model and orientation moving patterns of moths. (A) Physical construction of the 2D turbulent simulation model. It is 5 m in length and 3 m in width, and the mesh size is set as 0.02 m × 0.02 m. The odour source is set 0.6 m away from the left side. The air flow comes from the left side. The circles in the blue square represent the branches simulating the natural environment. (B) Physical construction of the 3D turbulent simulation model. It is 1.25 m in length, 0.1 m in height and 0.6 m in width, and the mesh size is set as 0.02 m × 0.02 m. The odour source is set 0.6 m away from the left side. The air flow comes from the left side. The circles in the blue square represent the branches simulating the natural environment. (C) The orientation behaviour model of a silkmoth.

Moreover, males in the upwind direction with higher-frequency pulse plumes (0.5 p/s and 1 p/s) travelled a significantly longer distance than did males in continuous clouds. Males in the latter group did not exhibit a significant increase in upwind flight distance compared to those in clean air. These findings suggest that fluctuations may play a crucial role in evoking flight behaviour. Some researchers have investigated antenna electroantennogram (EAG) recordings at different release frequencies. Increasing the pulse frequency resulted in the fusion of peaks [10]. These findings suggest that the limitations of moth olfactory neurons in responding to pulse tempos likely begin at the receptor level, indicating that different exposure times and frequencies within pheromone plumes may result in different orientation behaviours. In behavioural experiments, moths typically exhibit straight-line walking under high-frequency pheromone stimulation (e.g., 2 Hz), whereas they exhibit zigzag movement patterns under low frequencies (e.g., 0.5 Hz) (Fig. 1C) [11]. Collectively, these findings demonstrate that different stimulation frequencies can lead to distinct patterns of movement.

Researchers have investigated the flight patterns of moths to gain a deeper understanding of their pheromone-oriented behaviour [11]. In addition, researchers have analysed the walking patterns of male silkworm moths in a controlled wind tunnel environment via continuous pulsed stimulation at various frequencies with pheromones [12]. These findings revealed that zigzag turning is reset upon each administration of the new pheromone stimulation. Moths exhibit brief, straight movement along their body axis for less than 0.5 s, followed by zigzag turning. Upon losing pheromone detection ability, moths experience a short reaction period, during which they walk in a straight line along their body axis. This phase can be defined as the "reaction time." Different moth species exhibit varying reaction times when their sense of smell is impaired within a specific range [12–16]. The olfactory systems of male moths have evolved to locate conspecific females optimally by discerning their pheromone release frequencies. Therefore, searching within a certain frequency range is the most effective approach, particularly for long distances, which mimics natural circumstances with more complicated turbulence. In this context, the reaction time of male moths may be related to the female pheromone release frequency and orientation efficiency.

The delay in male moth orientation may also be influenced by varying pheromone concentrations. The estimated mean reaction concentration is 170 molecules [17]. In the simulation of the gypsy moth (*Lymantria dispar*), the threshold for the male response to pheromones was set at 4×10^4 molecules/cm^3 [18]. However, some researchers have suggested that adjustment of the odour reaction threshold and kinetics is influenced by the relative concentration ratios of intracellular Ca^{2+} and cyclic nucleotide levels. These factors synergistically regulate different ion channels [19]. Projection neurons (PNs) respond primarily to changes in odourant concentration rather than to the encoding of absolute concentration through pulse trains of stimulation [7]. Olfactory receptor neurons did not contribute to this response transformation; however, this was due to long-lasting inhibition affecting PNs in the antenna lobe (AL). The response threshold value may vary depending on the environment [20]. Therefore, the response threshold should also be considered a temporal parameter that can potentially affect orientation efficiency.

Researchers have proposed simulation models for eliciting moth navigation patterns. Celani et al. discussed physical constraints on signal transmission. These authors explained why pheromone release could create the time structure of the plume during turbulent flow [21]. Bau et al. [22] established four manoeuvres that are associated with the effectiveness of recontacting the plume. Researchers have conducted simulations for each behaviour and determined the optimal casting strategy. Liberzon et al. developed an orientation model for a universal turbulent environment and a flying moth tracing simulation model [23]. Others have explored the different orientations of pheromones and other resource-linked odours [24]. In addition, Jayaram et al. [25] discussed navigation mechanisms using frequency and intermittency as parameters in different environments and constructed a navigation function; others have also investigated the importance of the intermittency of turbulent flow in odour tracking [26]. Researchers have used a turbulent simulation model to specifically simulate the scales and transport of filaments [18]. Hernandez-Reyes et al. established a moth-based orientation model for mechanical practice [27]. Our study investigated the temporal dimension of navigation by integrating the hypothesis regarding "reaction time t_r" and explored the orientation algorithm constructed on the basis of the relationships among the reaction time, response threshold $\boldsymbol{\tau}$, release frequency, and wind velocity and how they interact with each other to influence orientation efficiency. Our objective was to propose an efficient algorithm for developing an orientation model. Our proposed navigation algorithm can potentially contribute to the odour-searching capabilities of robots, which could be utilized in improved monitoring of selected odour species.

2. Methods

2.1. Physical model construction

A chemical released at a source location undergoes manipulation through turbulent and molecular diffusion during advective transport by the wind. Turbulent dispersion dominates the odour dispersion process. The computational efficiency of this model is crucial because it requires many simulations. ANSYS FLUENT (ANSYS FLUENT 2020, ANSYS, Inc., Pennsylvania, USA) was used to simulate a turbulent environment. ANSYS FLUENT is general-purpose computational fluid dynamics (CFD) software used to model fluid flow and obtain different parameter series of each mesh after simulations, which could be useful for later agent orientation simulations as environmental support. A two-dimensional (2D) model was constructed, measuring 5 m in length and 3 m in width. The mesh size used was 0.02 m × 0.02 m, which referred to the width of the mesh hole as 0.02 m (Fig. 1A). The odour source was positioned 0.6 m from the left side. The wind velocity range of 0.3 m/s to 0.5 m/s was determined on the basis of previous experimental findings [7,9,12]. The pheromone was simulated to release from the odour source (Fig. 1) along the x-axis direction with a release velocity of 0.1 m/s via the ANSYS FLUENT/CFD species transport program, which is based on two-phase flow. The pheromone release frequency varied between 0.5 Hz and 4 Hz, and each release was sustained for 200 ms [9,12].

2.2. Simulation model construction

The fluctuating velocity gradients in turbulent flow create the spatial structure of the chemical field in complex patterns consisting of thin filaments. The distribution consisted of evoking peaks and valleys. The spatial characteristics depend on the physical nature of both the flow and the odourant [21]. Thus, the simulation of turbulent flow should include both release frequency changes and wind velocity changes. The simulation was conducted via a large-eddy simulation (LES) model and a species transport model (https://ansyshelp.ansys.com/account/secured?returnurl=/Views/Secured/corp/v202/en/flu_ug/flu_ug.html%23flu_ug). The LES model is widely recognized as an effective tool for simulating turbulence at larger lengths and time scales. The species transport model is used to solve conservation equations for chemical species, enabling the prediction of local mass fractions for each species by solving convection–diffusion equations. Here, we used species transport without a reaction model to solve the problem of volumetric reactions that occur during plume spreading during turbulent flow. Previous researchers have shown that efficiently operating with odour concentrations could be useful in computational models [28]. The mass fraction of species n, derived from the solution, represents the ratio of the mass of a particular species to the total mass of the mixture [21]. The 2D LES model can provide the required turbulence information [29], but several physical differences exist between the three-dimensional (3D) LES model and the 2D LES model [30]. To validate the reliability of the simulation data, a small 3D model was constructed, measuring 1.25 m in length, 0.6 m in width, and 0.1 m in height (Fig. 1B). The mesh dimensions were 0.02 m × 0.02 m, with a hole width of 0.02 m. When performing the calculations, we cut one face from a height of 0.05 m for discussion. To compare the 3D and 2D simulation results, a 2D model with the same dimensions and settings as the 3D model, which was 1.25 m in length and 0.6 m in width, was constructed. The simulation used three odour materials: bombykol, the primary component of the silk moth pheromone; cis-7,8-epoxy-2-methyloctadecane, the main constituent of the gypsy moth pheromone; and benzene, which was used for comparison (Table 2). The duration of the single release was 0.02 s. The turbulence intensity was set to 5 %, and the turbulent viscosity ratio was set to 10. The time step of the simulation was 0.01 s, and the process lasted 100 s.

2.3. Orientation model construction

The agent's movement mechanism, specifically the "reaction time," was determined through various simulations in turbulent environments (Figs. 1C and 2). The parameter settings were based on previous research (Table 1) [12]. The orientation simulation lasted for 100 s, with the agent ceasing its movement upon locating the source. An orientation completed within 100 s was considered successful. An orientation exceeding 100 s was considered either a failed case or an overtime case. The simulation was programmed via Python 3.0. Our analysis focused on different pheromone frequencies that varied at different points within a single case. The frequency decreased as the distance from the source increased.

2.4. Statistical methods

For the line charts of the odour mass concentration, the data were resampled 10 times, where each resample size was the same as the original data and standard deviations were computed and used by ANSYS-CFD-Post, which is a postprocessor that can enable visualization and quantitative analysis of the results of CFD simulations by creating graphical figures and postprocessing plots. The gap length distribution was computed by bootstrapping data from turbulent simulations of different conditions with different thresholds. The central tendency bars for gap length calculated under different conditions were computed via Python 3.0. Different moving

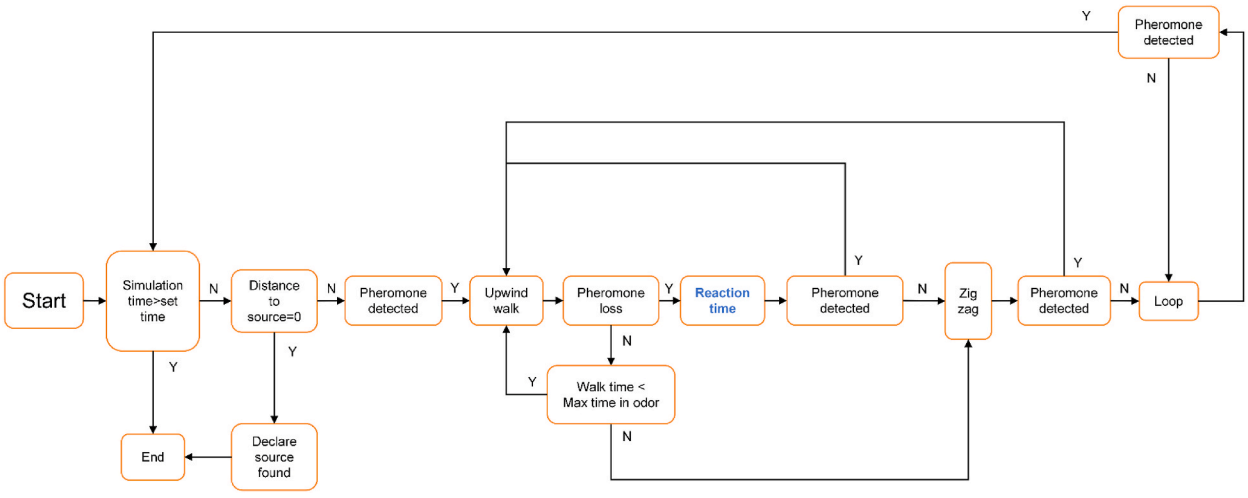

Fig. 2. Flowchart of the orientation algorithm of a silkmoth. The "reaction time" can be changed in this model to better understand the relationship with the orientation efficiency.

Table 1
The parameter settings of the orientation model. The moving agent is considered a point to simplify the calculation.

Walking velocity (m/s)	Zig-zag first turn (°)	Zig-zag Second turn (°)	Zig-zag third turn (°)	Loop turn rate (°/ms)	Reaction time tr (s)	Response threshold τ (mass fraction range)
0.025	68 ± 5	121 ± 10	132 ± 12	Random (0,0.1)	interim	0.02
Zig-zag first turn time (s)		Zig-zag second turn time (s)		Zig-zag third turn time (s)		Max time in odour (s)
1		1.5		1.9		5

Table 2
The molecular weights of different odour materials.

Odour	Bombykol	Cis-7,8-Epoxy-2-methyloctadecane	Benzene
Molecular weight (g/mol)	238.4	282.5	78.1

patterns during the orientation simulation were programmed and computed via Python 3.0. Different moving strategies were distinguished during the orientation simulation, and the positions and timings were recorded via Python 3.0. The orientation simulation for each condition was resampled 10 times, where each resample size was the same size as the original data and standard deviations were programmed and computed via Python 3.0.

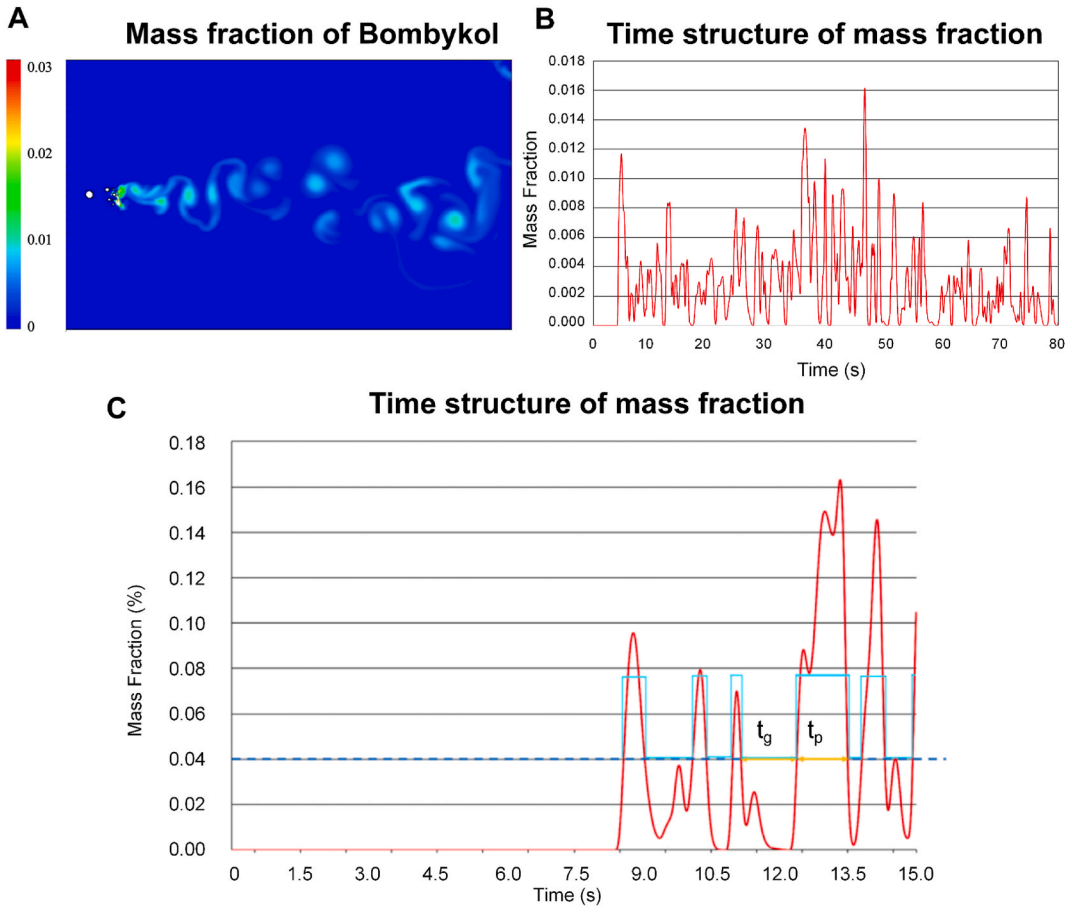

Fig. 3. An example of a turbulent simulation and time structure of the mass fraction. The simulation was performed at a wind velocity of 0.3 m/s, and the release frequency was 1 Hz. (A) The mass fraction map of bombykol. (B) Time structure of the mass fraction at the point 2 m downwind from the source. (C) Time structure of the mass fraction of the position 4 m away from the odour source. The threshold was set as 0.0004. The wind velocity is 0.5 m/s, and the odour release frequency is 1 Hz. The symbol t_g is the gap length, and t_p is the pulse length for a threshold $\tau = 0.0004$. The light blue line is the simplified time structure of the mass fraction for a threshold $\tau = 0.0004$.

3. Results

3.1. Turbulent flow simulation results

Turbulent simulations were conducted under different wind velocities of 0.3 m/s, 0.5 m/s, and 1 m/s and with different pheromone release frequencies of 1 Hz, 1.25 Hz, and 2 Hz. The mass fraction obtained from the solution represented the concentration of a species, defined as the mass of a species per unit mass of the mixture. We examined the solution mass fraction as a measure of the dispersion of odorous materials in fluid flow. The mass fraction was accurate for each mesh, and when the specific point was calculated, the closest mesh was used for discussion. As observed from the temporal structure at a specific distance from the source, the temporal information was concealed within the plume (Fig. 3B). A closer examination of the time structure of the mass fraction (Fig. 3C) revealed that the temporal characteristics can be determined by calculating the gap length of the time structure at a specific response threshold, which was set as 0.04 % mass fraction for comparison.

The time structure was simplified by determining the gap length of the mass fraction, which revealed limited temporal characteristics. Next, the gap length of the mass fraction was analysed under different conditions to assess the influences of different wind velocities, release frequencies, and distances from the source on the temporal characteristics of the plume (Fig. 4). We observed that altering the release frequency led to variations in the temporal characteristics of the mass fraction (Fig. 4A). As the release frequency increased, the gap length decreased. The temporal characteristics of the plume varied with the wind velocity (Fig. 4B). As the wind velocity increased, the gap length decreased. These findings indicate an inverse relationship between the wind velocity and gap length. Altering the distance from the source could also affect the temporal characteristics of the mass fraction of the odour (Fig. 4C). As the distance increased, the gap length increased, although not distinctly. Our findings revealed a direct relationship between distance and gap length, where greater distances corresponded to greater gap lengths. Additionally, the use of different odorous materials resulted in distinct temporal patterns in the mass fraction (Fig. 4D). Our findings revealed a direct relationship between molecular weight and gap length, with smaller molecular weights corresponding to shorter gap lengths. These findings indicated that the gap length could be

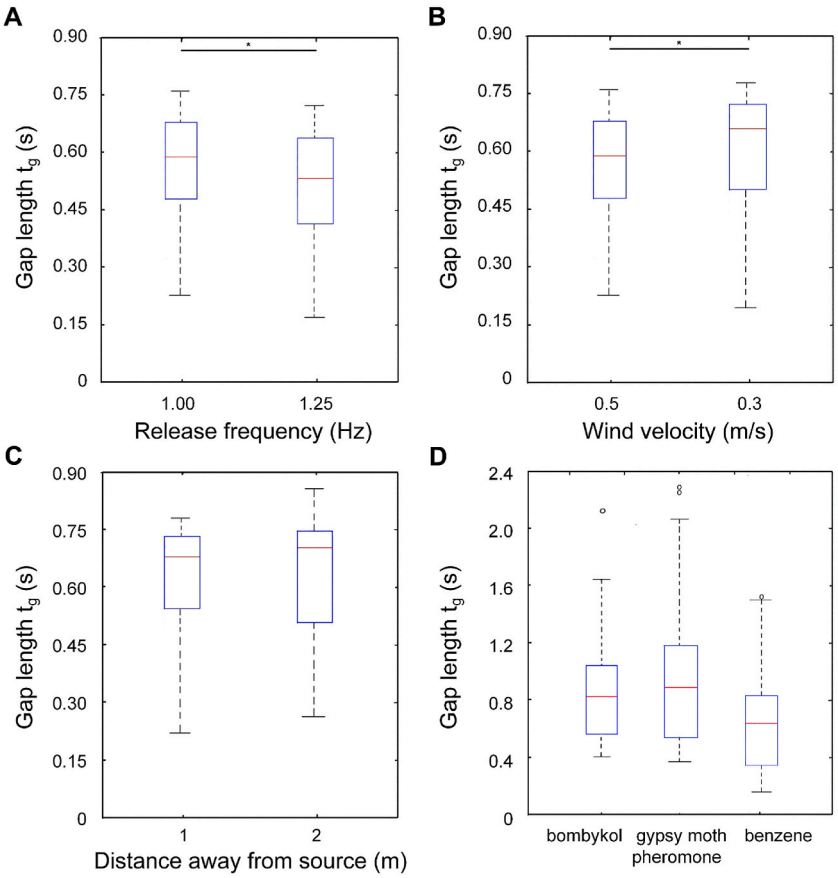

Fig. 4. Gap length calculated under different conditions. (A) Gap length at a position 1 m away from the odour source under different pheromone release frequencies: 1.25 Hz and 1 Hz. The wind velocity is 0.5 m/s, and $N = 10$. (B) Gap length 1 m away from the odour source under different wind velocities: 0.5 m/s and 0.3 m/s. The release frequency is 1 Hz, and $N = 10$. (C) Gap length under the same wind velocity of 0.3 m/s and a release frequency of 1 Hz from different distances away from the source, where $N = 10$. (D) Gap length under the same wind velocity of 0.3 m/s, release frequency of 1 Hz and distance of 1 m from the source with different odour stimuli ($N = 10$).

influenced by factors such as release frequency, wind velocity, distance from the source, and the type of odorous material used.

We also simulated the turbulent environment via both the 3D LES model and 2D LES model with the same plan area to compare their abilities to provide the necessary information for our study. Differences in the mass fractions of the time structures were observed between the two models. The 3D LES model demonstrated a smaller gap length than did the 2D LES simulation. Despite the loss of some detailed turbulence information, the 2D LES model could still accurately calculate the required temporal characteristics within the same range as the 3D model because both models exhibited the same range of gap lengths.

We assessed the effects of different release frequencies and wind velocities on the temporal characteristics of the plume, as well as how these characteristics changed with different response thresholds. The resulting gap length changes were analysed under different wind velocities and release frequencies along with response thresholds (Fig. 5). The findings indicated that varying the response thresholds resulted in different distributions of gap lengths at specific release frequencies (Fig. 5A–C). The gap length increased with response threshold and wind velocity (Fig. 5D–F). Next, we conducted orientation simulations under various conditions with different reaction times to examine the relationships among different wind velocities, release frequencies and distances from the source in combination with the reaction time. The findings indicated that orientation efficiency was influenced by both the reaction time and response threshold across various release frequencies. For example, at a release frequency of 1 Hz, the optimal orientation pattern occurred at a response threshold of 0.2 % and a reaction time of 0.8 s (Fig. 6A). The response threshold influenced the gap length distribution (Fig. 5). At a release frequency of 1 Hz, the gap length distribution under a response threshold of 0.2 % was within the same range as the optimal reaction time of approximately 0.8 s. Similar findings were observed at frequencies of 1.25 Hz (Fig. 6B) and 2 Hz (Fig. 6C). This suggested that when the gap length and reaction time were within a similar range, the orientation could be more optimal.

3.2. Orientation simulation results

To gain a deeper understanding of the orientation behaviour, especially the different trigger times for different moving strategies

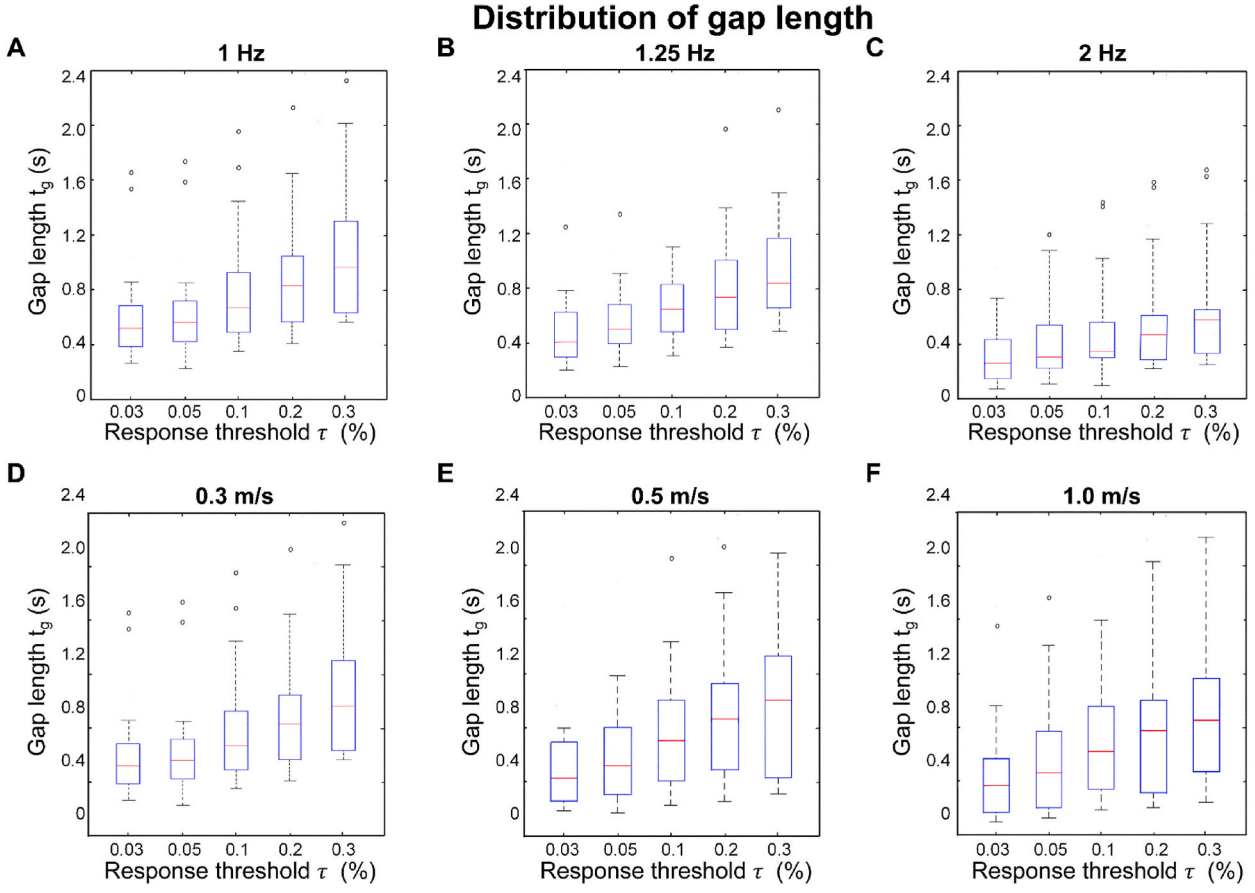

Fig. 5. Distribution of gap length under different conditions. (A)–(C) Gap length t_g under different thresholds τ of the time structure of the mass fraction 1 m downwind from the source with different release frequencies. The wind velocity is 0.3 m/s ($N = 10$). (D)–(F) Gap length t_g under different thresholds τ of the time structure of the mass fraction 1 m downwind from the source with different wind velocities. The release frequency is 1 Hz ($N = 10$).

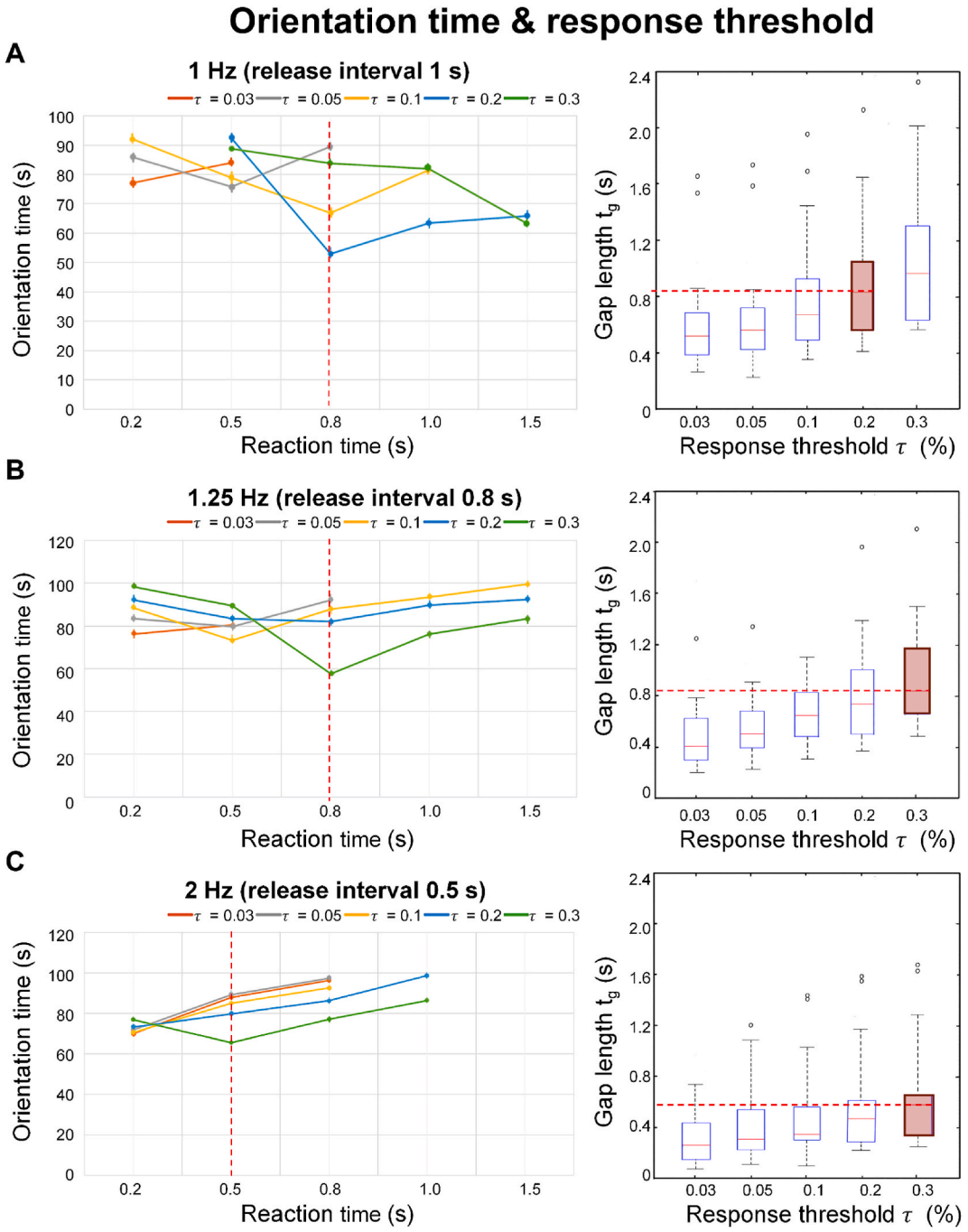

Fig. 6. The orientation simulation time and response thresholds. (A) The orientation simulation time at 1 Hz with different reaction times. The most efficient pattern is observed when the response threshold is 0.2 %, and the best reaction time is 0.8 s. Compared with the gap length distribution under a response threshold of 0.2 %, the reaction time and gap length are within the same range of values ($N = 10$). (B) The orientation simulation time at 1.25 Hz with different reaction times. The most efficient pattern is observed when the response threshold is 0.3 %, and the best reaction time is 0.8 s. Compared with the gap length distribution under a response threshold of 0.3 %, the reaction time and gap length are within the same range of values ($N = 10$). (C) The orientation simulation time at 2 Hz with different reaction times. The most efficient pattern is observed when the response threshold is 0.3 %, and the best reaction time is 0.5 s. Compared with the gap length distribution under a response threshold of 0.3 %, the reaction time and gap length are within the same range of values ($N = 10$).

and patterns such as straight walking, reaction time, zigzag turning, and looping, we conducted simulations and analysed the correlations between these behaviours. The findings demonstrated that the model successfully simulated the orientation behaviour. In some cases, efficient orientation was observed, whereas in others, a cyclical pattern emerged, which ultimately resulted in unsuccessful

orientation. We subsequently conducted simulations using consistent wind velocities of 0.3 m/s and 0.5 m/s and a release frequency varying from 0.5 Hz to 4 Hz while changing the reaction time parameter to determine its effect on orientation efficiency.

The simulation was conducted under the same conditions, including a wind velocity of 0.5 m/s, a release frequency of 0.5 Hz, and a starting position of 1 m from the odour source with different reaction times that were used in the simulation to elucidate differences in each search scenario (Fig. 7A). Here, we used 0.2 s, 0.5 s, 0.8 s, 1.0 s, 1.2 s, 1.5 s, and 2.0 s as different reaction times for the simulations. We calculated the reaction time-, zigzag turning-, and loop-triggered times for each case. These values were then compared (Table 3). The optimal orientation was observed at a reaction time of approximately 1.5 s. Excessive or insufficient reaction times resulted in orientation failure. In cases of failed orientation, the triggered times for the reaction time and zigzag turning were longer than those in successful cases. Next, a simulation was performed using a consistent wind velocity of 0.5 m/s, a different odour release frequency of 1 Hz, and a distance of 1 m from the source with different reaction times. We calculated the reaction time-, zigzag turning-, and loop-triggered times for each case. These values were then compared (Table 4). The findings indicated that optimal orientations were observed at reaction times of approximately 0.8 s or less. The optimal reaction time was within a range similar to that of the release interval, corresponding to the release frequency.

3.3. Orientation moving pattern distribution

We subsequently modified the wind velocity to examine its effect on the reaction time. The simulation was conducted under the same conditions, including a wind velocity of 0.3 m/s, a release frequency of 1 Hz, and a starting position of 1 m from the odour source (Fig. 7D–F). Different reaction times were used in the simulation to observe the variations in each search scenario. We calculated the reaction time-, zigzag turning-, and loop-triggered times for each case. These values were then compared to determine how their proportions differed in various cases (Table 5). The optimal orientation was achieved at a reaction time of approximately 0.9 s. Excessive or insufficient reaction times caused orientation failure. In the failed orientation cases, the triggered times for the reaction time and zigzag turning tended to be longer than those in the successful cases. Excessive or insufficiently triggered zigzag turning and reaction times could lead to inefficient orientation patterns. Compared with the results at a wind velocity of 0.5 m/s, the optimal reaction time appeared to be slightly longer owing to the different time structures that might be caused by different wind velocities.

We conducted additional simulations under different release frequencies and determined the zigzag turning-triggered times. A negative correlation was observed between the release frequency and zigzag turning-triggered time, corroborating the experimental findings that the moth would be most likely to trigger zigzag turning when it was in a higher release frequency environment [7,9,12].

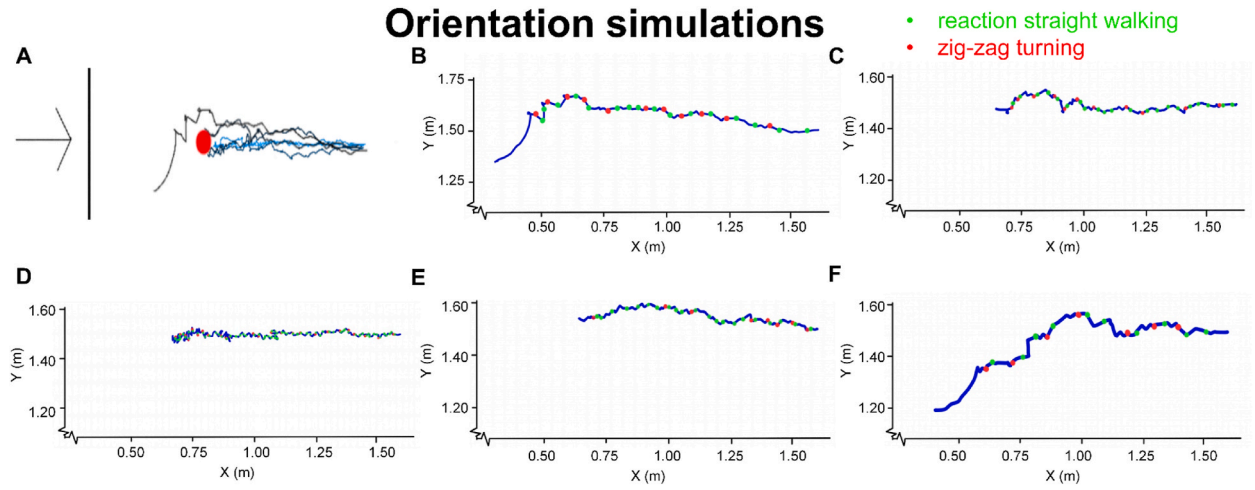

Fig. 7. Examples of orientation results. (A) Paths of the simulated agents under different reaction times at a wind velocity of 0.5 m/s and a release frequency of 0.5 Hz at a position 1 m away from the source with different reaction times. (B) The path of one failed orientation case with a reaction time of 2 s under a wind velocity of 0.5 m/s and a release frequency of 0.5 Hz at a position 1 m away from the source with different reaction times. The green dots represent the reaction time triggered time points, and the red dots represent the zigzag turning triggered time points. (C) Path of one successful orientation case with a reaction time of 1.5 s under a wind velocity of 0.5 m/s and a release frequency of 0.5 Hz at a position 1 m away from the source with different reaction times. The green dots represent the reaction time triggered time points, and the red dots represent the zigzag turning triggered time points. (D) Path of one overtimed orientation case with a reaction time of 0.1 s under a wind velocity of 0.3 m/s and a release frequency of 1 Hz at a position 1 m away from the source with different reaction times. The green dots represent the reaction time triggered time points, and the red dots represent the zigzag turning triggered time points. (E) Path of one successful orientation case with a reaction time of 0.9 s under a wind velocity of 0.3 m/s and a release frequency of 1 Hz at a position 1 m away from the source with different reaction times. The green dots represent the reaction time triggered time points, and the red dots represent the zigzag turning triggered time points. (F) Path of one failed orientation case with a reaction time of 2 s under a wind velocity of 0.3 m/s and a release frequency of 1 Hz at a position 1 m away from the source with different reaction times. The green dots represent the reaction time triggered time points, and the red dots represent the zigzag turning triggered time points.

Table 3
Orientation vs. reaction & movement trigger times under specific conditions. The orientation time differs with respect to different reaction times and trigger times of different movement strategies under a wind velocity of 0.5 m/s, a release frequency of 0.5 Hz, and a start position 1 m away from the source. $N = 10$.

Reaction time/s	0.2	0.5	0.8	1	1.2	1.5	2.0
Orientation time/s	failed	83.38	82.25	79.52	72.66	59.78	failed
Reaction straight walk trigger (time)	66.2	18.4	19.3	12.2	14.8	17.9	19.4
Zig-zag turning trigger (time)	28.4	13.2	5.1	7.5	8.8	11.7	10.3
Loop (time)	0.2	0	0	0	0	0	0.9

Table 4
Orientation time variation: impact of reaction & movement strategies under specific conditions. The orientation time differs as a result of different reaction times and the trigger times of different movement strategies under a wind velocity of 0.5 m/s, a release frequency of 1 Hz, and a start position 1 m away from the source. $N = 10$.

Reaction time/s	0.2	0.5	0.8	1	1.2	1.5
Orientation time/s	96.42	65.70	60.41	74.68	72.91	88.01
Reaction straight walk trigger (time)	29.4	21.3	18.9	14.2	14.5	16.2
Zig-zag turning trigger (time)	9.2	6.8	9.1	8.3	7.7	9.2
Loop (time)	0	0	0	0	0	0

Table 5
Orientation time variation: impact of reaction times and movement strategies under specific conditions. The orientation time differs as a result of different reaction times and the trigger times of different movement strategies under a wind velocity of 0.3 m/s, a release frequency of 1 Hz, and a start position 1 m away from the source. $N = 10$.

Reaction time/s	0.1	0.5	0.6	0.7	0.8	0.9	1.0	1.5	2.0
Orientation time/s	Over time	92.33	67.82	64.23	52.91	52.10	63.36	65.87	failed
Reaction straight walk trigger (time)	66.2	31.8	28.3	24.1	23.8	21.4	16.3	15.2	11.1
Zig-zag turning trigger (time)	24.2	18.1	15.2	14.4	10.7	10.3	11.9	12.2	6.8
Loop (time)	0	0	0	0	0	0	0	0	0.9

The agent walking model was used to simulate different movement patterns under different conditions. Odour detection was achieved by initiating searches from different locations oriented towards the source. With an appropriate reaction time, most agents reached this goal. Subsequently, simulations were conducted at certain release frequencies for different reaction times. Our findings indicated that different reaction times corresponded to distinct response thresholds, resulting in different gap length distributions. Higher pheromone release frequencies were associated with shorter reaction times than lower release frequencies.

4. Discussion

4.1. Investigation of the turbulent simulation and orientation simulation

In this study, we conducted 2D turbulence simulations. The physical model was constructed in a 2D format to accurately represent the walking behaviour of silk moths. The 2D model was sufficiently informative for subsequent analysis. An eddy simulation (LES) model was used to generate different turbulent flows. With respect to the silkmoth walking conditions, the chemical information was detected with high spatial accuracy by the antenna; thus, the pheromone conditions of a single point could be important in this discussion. The results reveal that the time scale of a single point can be used to construct a turbulent environment and convey temporal and spatial information. The species transition model was used to simulate odour diffusion. The mass fraction of the solution was used to evaluate the temporal characteristics of the plume. The simulation results revealed significant variations in odour frequency as the distance from the odour source increased, which was consistent with previous research on how odour information changes with distance [21]. The release frequency appeared to be less efficient than in the condition of laminar flow. However, the temporal structure of the plume, when located away from the odour source, retains distinct attributes associated with the different release frequencies. The release frequency affects certain aspects of the time structure but remains consistent with the release interval within a similar range, thereby conveying specific temporal information. Variations in the wind velocity led to alterations in the temporal patterns. This finding supports the inclusion of the wind velocity as a parameter for evaluation in the model. In addition, the distance from the source influences the temporal characteristics of the odour plume. However, it can be argued that the flow maintains consistent temporal characteristics over specific distances. This finding is consistent with those of previous studies. Baker. T. C. et al. [14] performed experiments to determine how the time structure of a pulsed plume could change with distance. They conducted experiments in the field with different wind velocities, released the pheromone from the source periodically and placed the antennae at different distances from the source. By detecting the EAG signals under different conditions, they reported that to maintain

high-amplitude bursts, the release frequency must be within a specific range according to the distance from the source. Rigolli, N. et al. [31] used machine learning algorithms to learn the relationship between odour and the distance from the source from a large dataset of examples. They reported that there was some connection between the input and output within certain distances, but when the distance increased, the efficacy varied with the dilution of the odour in space. This might indicate that more information or parameters should be considered when building the search model. Vickers N. J. et al. [15] conducted experiments to visualize the filaments of the pulsed released pheromone. They changed the release frequency from 10 pulses/s to 1 pulse/s in a wind tunnel measuring 1 m $\times$ 0.9 m $\times$ 3.65 m. They observed that these smoke filaments did appear to remain separate entities during passage through the length of their wind tunnel at all but the highest filament delivery rate in the study. These results suggested that the odour plume could maintain its structure within a rough range of distances over a broad range of release frequencies. This is somewhat similar to the pheromone release time structure under turbulent flow. The evidence in the turbulent simulations suggests that the interaction between the wind velocity, release frequency, and reaction time can significantly influence the search efficiency.

The simulation data suggest a relationship between the reaction time and search efficiency. As the release frequency increased, the optimal reaction time decreased. Furthermore, a higher wind velocity results in a shorter reaction time. Interestingly, we observed that the optimal reaction time can fall within a similar range as the release interval, which is determined by the release frequency and response threshold. This could be due to the optimal reaction time being aligned with the temporal characteristics of turbulent flow, thereby facilitating the use of the most efficient searching algorithm.

The turning strategy and moving pattern were simplified to focus on the reaction time. In addition, the agent was simplified to a point. However, this approach entails the loss of certain natural information compared with real moth behaviour. This may result in distortion in the moving simulation. Improving the agent simulation program could yield improved outcomes in elucidating the role of reaction time in efficient odour navigation.

The 2D LES model adequately captures the necessary temporal characteristics. The findings demonstrate that the simulation of a turbulent fluid in 2D closely resembles that in 3D. Although this approach is adequate for discussion, there are still some gaps in information. Simulation in a 3D environment enhances the precision and detail of the LES model owing to its inherent characteristics. The development of a suitable 3D model for turbulent simulations can improve the accuracy of the outcomes.

Turbulence was triggered by the model configuration. Branch structures are established in the model to facilitate the formation of distinct turbulent flow patterns. However, the input flow environment was simple. Experimentation with different flow environments or the introduction of random flow fluctuations can enhance the visual and dynamic characteristics of turbulent patterns, thereby creating a more realistic turbulent environment for agent simulations. Our investigations focused on the turbulent time structures of different odour materials and demonstrated their effects on both the orientation patterns and reaction times.

The orientation algorithm proposed in this study focuses primarily on the reaction time and response threshold. These parameters have potential utility in the development of a robotic system designed for locating an odour source. Researchers have suggested that at greater distances, normal material sensors could experience more encounters [32]. If it is possible to make good use of the correlation between the release interval and time threshold along with the reaction time in the moving process, it would lead to further utility in real orientation tasks. Studies have demonstrated that even in natural environments, random odour sources such as pheromones may not have specific release frequencies. However, as these odours disperse, they retain some frequency information. Moths can adjust their response thresholds to different odour concentrations under natural conditions [33]. Our algorithm enables mechanical adjustment of the response threshold to modify the gap length in accordance with the release frequency. By selecting values within the same range as the reaction time, it is possible to create an optimal orientation pattern under specific conditions. The inclusion of the orientation algorithm, which incorporates parameters such as the reaction time and response threshold, offers the potential to improve real navigation tasks within the search system.

4.2. Pros and cons

To highlight the strengths of our study, we first note that the results clearly demonstrated varying time thresholds across different wind velocities, release frequencies, and measurement distances, providing valuable insights into the dynamics of turbulent environments. Additionally, although the differences were not substantial enough to define specific relationships between similar conditions, they highlight important trends that warrant further investigation. Furthermore, incorporating extreme conditions in future studies could increase the practical applicability of the findings to more complex real-world scenarios. Finally, the orientation model based on the movement patterns of silkmoths, alongside findings related to similar behaviours in other species, such as Drosophila, which also react to pheromone loss [34], suggests the potential for broader applicability and improvements in orientation strategies.

On the other hand, our study also faces several limitations that must be addressed in future work. First, the limited simulation time (100 s for turbulent simulations and 120 s for orientation simulations) may have prematurely classified some scenarios as unsuccessful, potentially overlooking cases that might succeed with longer durations. This suggests the need for extended simulation periods to achieve more definitive results. Second, the minimal time variations among the successful cases were not sufficiently detailed for readers, indicating a need for clearer presentation and possibly more nuanced data analysis. Third, while the 2D simulation environment was effective, transitioning to a 3D model could significantly enhance the precision and detail of the LES model, better capturing the complex terrains and dynamics essential for more accurate orientation simulations. This shift could also facilitate the incorporation of real-time simulations alongside orientation tasks to better mimic and understand actual environmental conditions.

4.3. Pragmatic possibilities for use

The algorithm we used in the orientation model and the latent relationship between three temporal characteristics—the release interval, time threshold, and reaction time—could be used in future walking odour source navigation robotic systems to increase the search efficiency. Further study might uncover deeper connections and regulatory mechanisms within our proposed navigation algorithm, potentially enhancing its contribution to the odour-searching capabilities of robots and informing the development of improved monitoring strategies for selected odour species.

Ethics approval and consent to participate

Not applicable.

Consent for publication

Not applicable.

Funding

Not applicable.

Data availability statement

Data included in the article/supp. materials/referenced in the article are available at https://www.jianguoyun.com/p/DcLGckgQppPdDBil1tEFIAA.

CRediT authorship contribution statement

Yanting Liu: Writing – original draft. **Ryohei Kanzaki:** Supervision.

Declaration of competing interest

The authors declare that they have no known competing financial interests or personal relationships that could have appeared to influence the work reported in this paper.

Acknowledgements

We are deeply grateful and would like to extend our sincere thanks to Dr. Stephan Shuichi Haupt from The University of Tokyo Research Center for Advanced Science and Technology. His thoughtful suggestions and assistance in refining the article have been instrumental in enhancing its quality. We are truly appreciative of his generosity and expertise, and we are honored to have had his support throughout the process.

Appendix A. Supplementary data

Supplementary data to this article can be found online at https://doi.org/10.1016/j.heliyon.2024.e37004.

List of abbreviations

EAG	Electroantennogram
PN	Projection Neuron
AL:	Antenna Lobe
2D	two-dimensional
3D	three-dimensional
LES	Large Eddy Simulation

References

[1] N. Mohebbi, A. Schulz, T.L. Spencer, et al., The scaling of olfaction: moths have relatively more olfactory surface area than mammals, Integr. Comp. Biol. 1 (2022) 81–89, https://doi.org/10.1093/icb/icac006.

[2] M.F. Tariq, S.C. Sterrett, S. Moore, et al., Dynamics of odor-source localization: insights from real-time odor plume recordings and head-motion tracking in freely moving mice, bioRxiv (2023) 566539, https://doi.org/10.1101/2023.11.10.566539.
[3] S.P. Foster, K.G. Anderson, Sex pheromone biosynthesis, storage and release in a female moth: making a little go a long way, Proceedings of the Royal Society B 1941 (2020) 20202775, https://doi.org/10.1098/rspb.2020.2775.
[4] S.P. Foster, K.G. Anderson, J. Casas, Calling behavior and sex pheromone release and storage in the moth Chloridea virescens, J. Chem. Ecol. (2020) 10–20, https://doi.org/10.1007/s10886-019-01133-w.
[5] A. Mafra-Neto, R. Cardé, Effect of the fine-scale structure of pheromone plumes: pulse frequency modulates activation and upwind flight of almond moth males, Physiol. Entomol. 3 (1995) 229–242, https://doi.org/10.1111/j.1365-3032.1995.tb00006.x.
[6] W.E. Conner, T. Eisner, R.K. Vander Meer, et al., Sex attractant of an arctiid moth (Utetheisa ornatrix): a pulsed chemical signal, Behav. Ecol. Sociobiol. (1980) 55–63, https://doi.org/10.1007/BF00302519.
[7] T. Fujiwara, T. Kazawa, T. Sakurai, et al., Odorant concentration differentiator for intermittent olfactory signals, J. Neurosci. 50 (2014) 16581–16593, https://doi.org/10.1523/JNEUROSCI.2319-14.2014Annual.
[8] J. Murlis, M.A. Willis, R.T. Cardé, Spatial and temporal structures of pheromone plumes in fields and forests, Physiol. Entomol. 3 (2000) 211–222, https://doi.org/10.1046/j.1365-3032.2000.00176.x.
[9] T. Baker, M. Willis, K. Haynes, P. Phelan, A pulsed cloud of sex pheromone elicits upwind flight in male moths, Physiol. Entomol. 3 (1985) 257–265, https://doi.org/10.1111/j.1365-3032.1985.tb00045.x.
[10] J. Bau, K.A. Justus, R.T. Cardé, Antennal resolution of pulsed pheromone plumes in three moth species, J. Insect Physiol. 4 (2002) 433–442, https://doi.org/10.1016/S0022-1910(02)00062-8.
[11] T. Baker, Upwind flight and casting flight: complementary phasic and tonic systems used for location of sex pheromone sources by male moth, Proc. 10th Int. Symp. Olfaction and Taste, Oslo (1990) 10029602642.
[12] K. Ryohei, S. Naoko, S. Tatsuaki, Self-generated zigzag turning of Bombyx mori males during pheromone-mediated upwind walking, Zool. Sci. 3 (1992) 515–527. https://www.cabidigitallibrary.org/doi/full/10.5555/19931178744.
[13] T. Baker, R. Vogt, Measured behavioural latency in response to sex-pheromone loss in the large silk moth Antheraea polyphemus, J. Exp. Biol. 1 (1988) 29–38, https://doi.org/10.1242/jeb.137.1.29.
[14] T.C. Baker, K. Haynes, Field and laboratory electroantennographic measurements of pheromone plume structure correlated with oriental fruit moth behaviour, Physiol. Entomol. 1 (1989) 1–12, https://doi.org/10.1111/j.1365-3032.1989.tb00931.x.
[15] N.J. Vickers, T.C. Baker, Male Heliothis virescens maintain upwind flight in response to experimentally pulsed filaments of their sex pheromone (Lepidoptera: noctuidae), J. Insect Behav. (1992) 669–687, https://doi.org/10.1007/BF01047979.
[16] T.L. Stepien, C. Zmurchok, J.B. Hengenius, et al., Moth mating: modeling female pheromone calling and male navigational strategies to optimize reproductive success, Appl. Sci. 18 (2020) 6543, https://doi.org/10.3390/app10186543.
[17] K.-E. Kaissling, E. Priesner, Die riechschwelle des seidenspinners, Naturwissenschaften (1970) 23–28, https://doi.org/10.1007/BF00593550.
[18] J.A. Farrell, J. Murlis, X. Long, et al., Filament-based atmospheric dispersion model to achieve short time-scale structure of odor plumes, Environ. Fluid Mech. (2002) 143–169, https://doi.org/10.1023/A:1016283702837.
[19] M. Stengl, Pheromone transduction in moths, Front. Cell. Neurosci. (2010) 133, https://doi.org/10.3389/fncel.2010.00133.
[20] F. Koutroumpa, C. Monsempès, S. Anton, et al., Pheromone receptor knock-out affects pheromone detection and brain structure in a moth, Biomolecules 3 (2022) 341, https://doi.org/10.3390/biom12030341.
[21] A. Celani, E. Villermaux, M. Vergassola, Odor landscapes in turbulent environments, Phys. Rev. X 4 (2014) 041015, https://doi.org/10.1103/PhysRevX.4.041015.
[22] J. Bau, R.T. Cardé, Modeling optimal strategies for finding a resource-linked, windborne odor plume: theories, robotics, and biomimetic lessons from flying insects, Integr. Comp. Biol. 3 (2015) 461–477, https://doi.org/10.1093/icb/icv036.
[23] A. Liberzon, K. Harrington, N. Daniel, et al., Moth-inspired navigation algorithm in a turbulent odor plume from a pulsating source, PLoS One 6 (2018) e0198422, https://doi.org/10.1371/journal.pone.0198422.
[24] R.T. Cardé, Navigation along windborne plumes of pheromone and resource-linked odors, Annu. Rev. Entomol. (2021) 317–336, https://doi.org/10.1146/annurev-ento-011019-024932.
[25] V. Jayaram, N. Kadakia, T. Emonet, Sensing complementary temporal features of odor signals enhances navigation of diverse turbulent plumes, Elife (2022) e72415, https://doi.org/10.7554/eLife.72415.
[26] B.T. Michaelis, K.W. Leathers, Y.V. Bobkov, et al., Odor tracking in aquatic organisms: the importance of temporal and spatial intermittency of the turbulent plume, Sci. Rep. 1 (2020) 7961, https://doi.org/10.1038/s41598-020-64766-y.
[27] C.A. Hernandez-Reyes, S. Fukushima, S. Shigaki, et al., Identification of exploration and exploitation balance in the silkmoth olfactory search behavior by information-theoretic modeling, Front. Comput. Neurosci. (2021) 629380, https://doi.org/10.3389/fncom.2021.629380.
[28] M. Schmuker, V. Bahr, R. Huerta, Exploiting plume structure to decode gas source distance using metal-oxide gas sensors, Sensor. Actuator. B Chem. (2016) 636–646, https://doi.org/10.1016/j.snb.2016.05.098.
[29] D. Bouris, G. Bergeles, 2D LES of vortex shedding from a square cylinder, J. Wind Eng. Ind. Aerod. 1–2 (1999) 31–46, https://doi.org/10.1016/S0167-6105(98)00200-1.
[30] L. Shi, G. Yang, S. Yao, Large eddy simulation of flow past a square cylinder with rounded leading corners: a comparison of 2D and 3D approaches, J. Mech. Sci. Technol. (2018) 2671–2680, https://doi.org/10.1007/s12206-018-0524-y.
[31] N. Rigolli, N. Magnoli, L. Rosasco, A. Seminara, Learning to predict target location with turbulent odor plumes, Elife (2022), https://doi.org/10.7554/eLife.72196.
[32] S.D. Boie, E.G. Connor, M. McHugh, et al., Information-theoretic analysis of realistic odor plumes: what cues are useful for determining location? PLoS Comput. Biol. 7 (2018) e1006275 https://doi.org/10.1371/journal.pcbi.1006275.
[33] Y. Liu, J.J. Heath, S. Zhang, et al., A mosaic of endogenous and plant-derived courtship signals in moths, Curr. Biol. 16 (2023) 3529–3535. e4, https://doi.org/10.1016/j.cub.2023.07.010.
[34] M. Demir, N. Kadakia, H.D. Anderson, et al., Walking Drosophila navigate complex plumes using stochastic decisions biased by the timing of odor encounters, Elife (2020) e57524, https://doi.org/10.7554/eLife.57524.